[Mn(III)(2-OHsalpn)]$_2$ Is an Efficient Functional Model for the Manganese Catalases

Andrew Gelasco and Vincent L. Pecoraro*

Department of Chemistry
The University of Michigan
Ann Arbor, Michigan 48019-1055

Received May 17, 1993

Manganese catalases use a dinuclear active site to catalyze the disproportionation of hydrogen peroxide to dioxygen and water. A low-resolution structure of the *Thermus thermophilus* enzyme demonstrates that two manganese ions are in close proximity (≈3.6 Å).[1] EPR spectroscopy confirms that the manganese ions are weakly exchange-coupled in the Mn(II)$_2$ and Mn(II/III) forms[2] and more strongly coupled in the Mn(III/IV) enzyme.[2,3] Optical absorption spectra have been used as evidence to support a bis-μ-carboxylato μ-oxo-bridged structure for the Mn(III)$_2$ enzyme. A minimal catalytic mechanism that has the enzyme cycle between Mn(II)$_2$ and Mn(III)$_2$ forms has been proposed by Penner-Hahn for the catalytic cycle.[3]

Functional models for the Mn catalases employing the enzymatic oxidation cycle [Mn(II)$_2$/Mn(III)$_2$] are not widely known. In fact, the only model system utilizing a dinuclear Mn(II)$_2$/Mn(III)$_2$ cycle has not been crystallographically characterized and loses activity after several hundred turnovers.[4] Other catalase models, although quite efficient, cycle between higher oxidation levels.[5] Herein we report the first crystallographically characterized dinuclear Mn model that approaches some of the structural, spectroscopic, and functional properties of the Mn catalases. Furthermore, we present the first functional catalase model in which both the oxidized and reduced forms have been isolated.

Previous studies[6,7] have demonstrated various geometries possible for Mn(III) complexes of the ligand 2-OHsalpn (1,3-bis(salicylideneimino)-2-propanol). In the study of the chemistry of low-valent complexes of this ligand, a new structural class was discovered containing a μ_2-alkoxo core with symmetric Mn ion environments. The complex Na$_2$[Mn(II)(2-OHsalpn)]$_2$·2CH$_3$OH (**1**) was prepared and isolated as a yellow powder by the reaction of the ligand 2-OHsalpn with 3 equiv of NaOMe and 1 equiv of Mn(ClO$_4$)$_2$·6H$_2$O in methanol using standard Schlenk techniques.[8] This complex can be oxidized by O$_2$ in acetonitrile to give the corresponding symmetric Mn(III)$_2$ dimer, [Mn(III)(2-OHsalpn)]$_2$ (**2**).[9] An ORTEP diagram of a ring-substituted derivative of **2**, [Mn(III)(2-OH(5-NO$_2$-sal)pn)]$_2$ (**3**) is shown in Figure 1,[10] with important bond distances and angles given in the figure caption. Because there is no donating solvent present and the Jahn-Teller axis is oriented symmetrically through the bridging core, the complex can maintain a symmetric geometry. In contrast, crystallization of **1** from methanol in air yields the previously described asymmetric dimer [Mn(III)$_2$(2-OHsalpn)$_2$·CH$_3$OH] (**4**).[6] The conversion from symmetric to asymmetric dimer leads to a marked alteration of the Mn-Mn distances as **1**, **2**, and **4** show 3.10-,[11] 3.23-, and 3.81-Å separations, respectively.

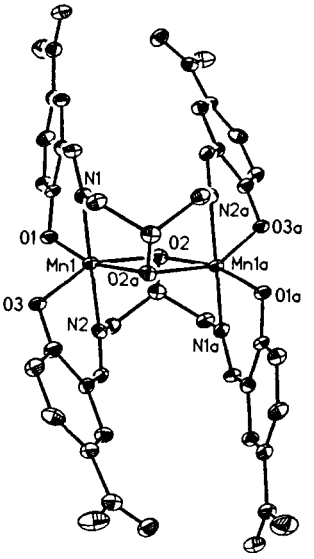

Figure 1. ORTEP diagram of [Mn(III)(2-OH(5-NO$_2$-sal)pn)] **3**) with themral ellipsoids shown at 50% probability. Important distances (Å); Mn1-Mn1a 3.229(2), Mn1-O1 1.904(3), Mn1-O2 2.331(3), Mn1-O3 2.096(3), Mn1-O2a 1.923(3), Mn1-N1 1.968(2), Mn1-N2 2.017(2); and angles (deg); Mn1-O2-Mn1a 99.91(1), O1-Mn1-O2 87.8(1), O1-Mn1-O3 105.7(1), O1-Mn1-N1 89.1(1), O1-Mn1-N2 93.2(1), O2-Mn1-N1 108.2(1), O2-Mn1-N2 72.7(1), O2-Mn1-O2a 80.9(1), O3-Mn1-O2a 89.1(1), O3-Mn1-N1 94.0(1), O3-Mn1-N2 84.7(1), O2a-Mn1-N1 82.5(1), O2a-Mn1-N2 95.5(1).

The reaction of H_2O_2 with **1** or **2** in acetonitrile causes the evolution of oxygen (and water) and a cycling between the Mn(II)$_2$ and Mn(III)$_2$ oxidation states for the complexes. The addition of 1 equiv of H_2O_2 to **1** shows isosbestic conversion to **2** and vice versa. Oxygen evolution experiments indicate that these complexes can complete the catalase reaction for at least 1000 turnovers without significant decomposition of the catalyst. Isolation of dioxygen after the addition of $H_2{}^{18}O_2$ yields exclusively $^{18}O_2$. If $H_2{}^{18}O_2$ and $H_2{}^{16}O_2$ are added simultaneously to either manganese complex, $^{18}O_2$ and $^{16}O_2$ are recovered but no $^{16,18}O_2$ is detected. This isotope labeling pattern follows the isotopic O$_2$ composition shown for the *Lactobacillus plantarum* catalase.[12] The reaction of H_2O_2 with a 50:50 mixture of **1** and [Mn(II)(2-OH(5-NO$_2$-sal)pn)]$_2^{2-}$ gives mass peaks for the recovered material only for **2** and **3**, and not for [Mn(III)$_2$(2-OHsalpn)-

(1) (a) Barynin, V. V.; Grebenko, A. I. *Dokl. Akad. Nauk SSSR* **1986**, *286*, 461-464. (b) Barynin, V. V.; Vagin, A. A.; Melik-Adamyan, V. R.; Grebenko, A. I.; Khangulov, S. V.; Popov, A. N.; Andrianova, M. E.; Vainshtein, B. K. *Dolk. Akad. Nauk SSSR* **1986**, *288*, 877-880.

(2) Khangulov, S. V.; Voyevodskaya, N. V.; Barynin, V. V.; Grebenko, A. I.; Melik-Adamyan, V. R. *Biofizika* **1987**, *32*, 960-966.

(3) Penner-Hahn, J. E. In *Manganese Redox Enzymes*; V. L. Pecoraro, Ed.; VCH Publishers, Inc.: New York, 1992; pp 29-45.

(4) Mathur, P.; Crowder, M.; Dismukes, G. C. *J. Am. Chem. Soc.* **1987**, *109*, 5227-5233.

(5) (a) Larson, E. J.; Pecoraro, V. L. *J. Am. Chem. Soc.* **1991**, *113*, 7809-7810. (b) Larson, E. J.; Pecoraro, V. L. *J. Am. Chem. Soc.* **1991**, *113*, 3810-3818. (c) Naruta, Y.; Maruyama, K. *J. Am. Chem. Soc.* **1991**, *113*, 3595-3596. (d) Sakiyama, H.; Okawa, H.; Isobe, R. *J. Chem. Soc., Chem. Commun.* **1993**, 882-884.

(6) (a) Bonadies, J. A.; Kirk, M. L.; Lah, M. S.; Kessissoglou, D. P.; Hatfield, W. E.; Pecoraro, V. L. *Inorg. Chem.* **1989**, *28*, 2037-2044. (b) Bonadies, J. A.; Maroney, M. J.; Pecoraro, V. L. *Inorg. Chem.* **1989**, *28*, 2044-2051.

(7) Bertoncello, K.; Fallon, G. D.; Murray, K. S.; Trekink, E. R. T. *Inorg. Chem.* **1991**, *30*, 3056.

(8) Analysis for **1** (Mn$_2$C$_{34}$H$_{30}$N$_4$O$_6$Na$_2$·2CH$_3$OH). Calcd: C, 53.4; H, 4.49; N, 6.93; Mn, 13.59; Na, 5.69. Found: C, 53.1; H, 4.67; N, 6.89; Mn, 13.6; Na, 5.28. FAB mass spectrometry: FAB$^-$ spectrum gives molecular ion peak for [Mn(II)(2-OHsalpn)]H$^-$ = 701. Room temperature magnetic moment = 5.68 μ_B. A DMF solution of **1** shows a classic X-band EPR spectrum for a Mn(II) dimer as described in ref 4 (Figure S4).

(9) Analysis for **2** (Mn$_2$C$_{34}$H$_{30}$N$_4$O$_6$). Calc: C, 58.3; H, 4.32; N, 8.00; Mn, 15.7. Found: C, 57.9; H, 4.41; N, 7.89; Mn, 15.6. Mass spectrometry: FAB$^+$ spectrum gives molecular ion peak for [Mn(III)(2-OHsalpn)] = 700. Room temperature magnetic moment = 4.71 μ_B.

(10) X-ray parameters for **3**: [Mn(III)(2-OH(5-NO$_2$salpn)]$_2$, Mn$_2$C$_{34}$H$_{26}$N$_8$O$_{14}$, MW 880.52; crystal system, monoclinic ($P2_1/n$); a = 10.562(2), b = 14.084(4), and c = 12.655(2) Å; β = 113.19(1)°; V = 1730 Å^3; Z = 2; d_{obsd} = 1.69 g/cm^3; d_{calcd} = 1.68 g/cm^3; crystal dimensions, 0.21 × 0.22 × 0.15 mm^3; Mo Kα 0.7107 Å; T = 145 K; Siemens R3m/v four-circle diffractometer. Data were reduced using the SHELXTL PLUS program package on a VAXstation 3500; all non-hydrogen atoms were refined anisotropically. Hydrogen atoms were located from difference Fourier map, with isotropic thermal parameters refined using a riding model, U = 1.2($U_{eq}C$). μ = 7.8 cm^{-1}; $5 < 2\theta < 52°$; unique reflections = 3415, no. of parameters = 301; reflections with $I > 2\sigma(I)$ = 2770; R = 0.0591, R_w = 0.0602.

(11) Riggs, P. J.; Penner-Hahn, J. E., personal communication.

(12) Waldo, G. S. Ph.D. Thesis, University of Michigan, 1991.

0002-7863/93/1515-7928$04.00/0

Table I. Initial Rate Data for Mn Catalase and Mn Models[a]

catalyst	rate (s^{-1})
L. plantarum Mn catalase	2×10^5
Na [Mn(II)(2-OH(3,5-Cl-sal)pn)]$_2$	11.0 ± 0.9
[Mn(III)(2-OH(3,5-Cl-sal)pn)]$_2$	10.0 ± 0.8
[Mn(III)(2-OH(5-Cl-sal)pn)]$_2$	12.4 ± 0.5
Na_2[Mn(II)(2-OH(5-Cl-sal)pn)]$_2$	13.1 ± 0.4
[Mn(III)(2-OHsalpn)]$_2$	13.0 ± 1.1
[Mn(III)(2-OH(5-NO_2-sal)pn)]$_2$	11.2 ± 0.5
Mn(II)(ClO_4)$_2$·6H_2O	$(6.25 \pm 1.5) \times 10^{-3}$

[a] Conditions: [H_2O_2] = 133 mM, [catalyst] = 111 μM.

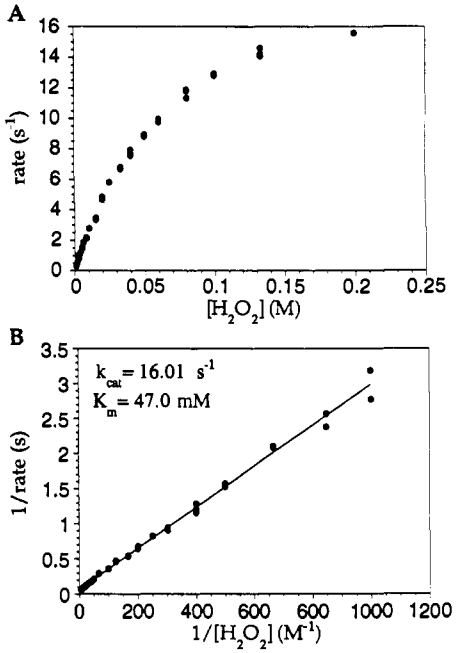

Figure 2. (A) Rate of H_2O_2 disproportionation vs H_2O_2 concentration in acetonitrile. The plot shows saturation kinetics for Na_2[Mn_2(2-OH-(5-Cl-sal)pn)]$_2$. (B) Lineweaver–Burke plot (double reciprocal plot) of the data in part A.

(2-OH(5-NO_2-sal)pn)]. This provides strong evidence that the dimers are not dissociating into monomers during the catalytic process.

The initial rate of reaction of these complexes with H_2O_2 was determined using a modified Clark-type O_2 electrode. Table I compares the initial rate of H_2O_2 disproportionation by different derivatives of **1** and **2**. The complex [Mn(III)$_2$(2-OH(5-Cl-sal)-pn)$_2$] (**5**) exhibits saturation kinetics as shown in Figure 2A. Figure 2B presents these data in a double reciprocal (Lineweaver–Burke) plot, demonstrating a linear relationship from which k_{cat} (16 ± 3 s^{-1}) and K_m (47 ± 10 mM) may be extracted. In comparison, the Mn catalase from *L. plantarum*[3] has a K_m = 200 mM and $k_{cat} = 2 \times 10^5$ s^{-1}, while Mn(II)(ClO_4)$_2$ has a $k_{cat} = 6.3 \times 10^{-3}$ s^{-1}. Relative values for k_{cat}/K_m for the Mn catalase and **5** are 1×10^6 and $(3.5 \pm 0.2) \times 10^2$ M^{-1} s^{-1}, respectively, indicating that the enzyme is approximately 3000 times more efficient than our synthetic catalyst. The *L. plantarum* catalase was initially described as azide insensitive; however, this enzyme can be inhibited by azide at high concentrations, with the pH-dependent K_i = 80 mM at pH = 7.[3] The catalase activity of **5** is not inhibited in acetonitrile to saturating concentrations of azide (≈50 mM).

Hydroxylamine is another peroxide analogue that has been used as a probe of enzyme activity. In the absence of H_2O_2, the enzyme is reduced to the Mn(II)$_2$ form by NH_2OH. However, if H_2O_2 is present, the enzyme is trapped in a catalytically inactive, superoxidized Mn(III,IV) state.[13] Treatment with NH_2OH in the absence of H_2O_2 will slowly regenerate the reduced form and restore catalytic activity.[14] It is most likely that NH_2OH, unlike H_2O_2, reduces the enzyme by only one electron. If this is done in the Mn(III)$_2$ oxidation level, an intermediate Mn(II,III) enzyme should be formed. If the next molecule to bind is NH_2OH, then the enzyme will be reduced to Mn(II)$_2$ and the cycle can be continued. However, if H_2O_2 binds next, the enzyme will be oxidized by two electrons to the Mn(III,IV) form. Since reduction of the Mn(III,IV) enzyme by hydroxylamine is slow, this superoxidized level will eventually be the dominant species. The [Mn(II)(2-OHsalpn)]$_2^{2-}$ system can also be driven to a catalytically inactive Mn(III,IV) species that has an EPR spectrum[15] (Figure S4) that is strikingly similar to that of the superoxidized Mn catalase.[13] This molecule can be reduced to a catalytically active species through NH_2OH reduction.

In summary, the [Mn(III)(2-OHsalpn)]$_2$ system cycles between the Mn(II)$_2$ and Mn(III)$_2$ oxidation levels, maintaining its dinuclear integrity throughout the process. It shows respectable turnover rates, exhibits saturation kinetics with H_2O_2, is reasonably stable (showing greater than 1000 turnovers), has the same $^{18}O_2$ labeling as the enzyme, is azide insensitive under conditions that the manganese catalase is not inhibited by azide, and forms a catalytically inactive Mn(III,IV) form (with an almost identical EPR spectrum to that of the enzyme) that can be reduced to a catalytically active state by NH_2OH.

Acknowledgment. The authors thank Ms. Pamela Riggs, Mr. Tim Stemmler, and Prof. James Penner-Hahn for allowing us to use unpublished data. This work was funded by NIH (GM39406).

Supplementary Material Available: Tables containing complete crystallographic data for **3**, including all bond lengths and angles and anisotropic thermal parameters, and the complete numbering scheme (Figure S3) for the complex; the EPR spectra of [Mn(II)(2-OHsalpn)]$_2^{2-}$ (Figure S4) and of Mn catalase and synthetic models (Figure S5) (11 pages); listing of calculated and observed structure factors for **3** (13 pages). Ordering information is given on any current masthead page.

(13) Fronko, R. M.; Penner-Hahn, J. E.; Bender, C. J. *J. Am. Chem. Soc.* **1988**, *110*, 7554–7555.
(14) Waldo, G. S.; Fronko, R. M.; Penner-Hahn, J. E. *Biochemistry* **1991**, *30*, 10486–10490.
(15) It is important to note that the EPR spectrum of the Mn(III/IV) complex is dramatically different from that of the asymmetric complex [Mn(III/IV)(2-OHsalpn)$_2$THF]$^+$ described in Larson, E.; Haddy, A.; Kirk, M. L.; Sands, R. H.; Hatfield, W. E.; Pecoraro, V. L. *J. Am. Chem. Soc.* **1992**, *114*, 6263–6265.